IDYNO: Learning Nonparametric DAGs from Interventional Dynamic Data

Anonymous Authors¹

Abstract

000

002

008 009 010

012

015

018

019

020

021

025

028

029

030

034

035

036

037

038

039

041

043

044

045

046

047

049

050

051

052

053

054

Causal discovery in the form of a directed acyclic graph (DAG) for time series data has been widely studied in various domains. The resulting DAG typically represents a dynamic Bayesian network (DBN), capturing both the instantaneous and timedelayed relationships among variables of interest. We propose a new algorithm, IDYNO, to learn the DAG structure from potentially nonlinear times series data by using a continuous optimization framework that includes a continuous acyclicity constraint. The proposed algorithm is designed to handle both observational and interventional time series data. We demonstrate the promising performance of our method on synthetic benchmark datasets against state-of-the-art baselines. In addition, we show that the proposed method can more accurately learn the underlying structure of a sequential decision model, such as a Markov decision process, with a fixed policy in typical continuous control tasks.

1. Introduction & Related Work

Probabilistic graphical models (Pearl, 1988; Koller & Friedman, 2009; Pearl, 2009) have been widely adopted in applications of artificial intelligence since the 1990s. Dynamic probabilistic graphical models are particularly applicable in real-world problems, such as for neuroscience (Rajapakse & Zhou, 2007), molecular biology (Linzner et al., 2019), and computer vision (Meng et al., 2018) tasks, since they capture dynamics in temporal data like time series by explicitly modeling how variables change over time.

Perhaps the most popular dynamic graphical models in the literature are dynamic Bayesian networks (DBNs) (Dean & Kanazawa, 1989; Murphy, 2002), which are discrete-time

Preliminary work. Under review by the International Conference on Machine Learning (ICML). Do not distribute.

models with an underlying directed acyclic graph (DAG) structure (e.g. Figure 1). While initial work in DBNs considered discrete variables, there has been plenty of subsequent literature on models with continuous variables, which are more appropriate for time series data involving continuousvalued measurements. For instance, DBNs can represent structured vector auto-regressive (SVAR) models from the statistics and econometrics literature (Reale & Wilson, 2001; 2002; Demiralp & Hoover, 2003; Swanson & Granger, 1997; Lanne et al., 2017; Kilian, 2013; Tank et al., 2019). Note that there are other related dynamic probabilistic graphical models for (discrete-time) time series data (Eichler, 1999; Dahlhaus, 2000) as well as for a parallel stream of research on continuous-time graphical models (Nodelman et al., 2002; Didelez, 2008; Gunawardana et al., 2011; Meek, 2014; Bhattacharjya et al., 2018).

Typical learning tasks for graphical models include parameter estimation and graph structure discovery. Structure discovery for both static and dynamic models aims at learning the graphical structure underlying the probabilistic model, usually in the form of a DAG. Standard structure learning methods can be categorized as scorebased, constraint-based, or hybrid methods that combine the approaches. Score-based DAG learning methods find a graphical model that best fits the data while also controlling the complexity of the DAG, according to a scoring function (Heckerman et al., 1995; Chickering, 2002). On the other hand, constraint-based methods identify a structure that conforms to conditional independencies between variables as gauged by statistical tests (Spirtes et al., 2001; Tsamardinos et al., 2006; Colombo et al., 2012; Malinsky & Spirtes, 2019). Structure learning methods of both basic types are often super-exponential in complexity due to a combinatorial search over all possible graphs.

To address computational issues, there has been a recent trend towards score-based approaches for models involving continuous variables that formulate a more tractable continuous optimization problem (Zheng et al., 2018). Several works have since successfully extended the initially proposed formulation to nonlinear as well as nonparametric models (Yu et al., 2019; Lachapelle et al., 2020; Kalainathan et al., 2018; Ng et al., 2019; Zheng et al., 2020).

¹Anonymous Institution, Anonymous City, Anonymous Region, Anonymous Country. Correspondence to: Anonymous Author <anon.email@domain.com>.

It is well known that structure discovery for DAGs with *observational* data alone, i.e. independent and identically distributed (i.i.d.) samples from a joint distribution over all random variables, does not necessarily provide the entire DAG structure (Spirtes et al., 2001; Pearl, 2009; Peters & Bühlmann, 2014; Oates et al., 2016); the structure can only be identified up to a Markov equivalence class in general, if one makes further assumptions.

058

059

060

061

062

063

064

065

066

067

068

069

070

075

076

078

079

081

082

083

086

087

088

089

090

091

092

093

094

095

096

097

098

099

100

104

105

106

109

The gold standard for causal discovery is achieved when one can perform experiments by intervening in a system and measuring the ramifications. This results in *interventional* data, which provides additional information that could potentially identify the underlying DAG structure. With a sufficient number of interventions, DAGs are fully identifiable (Eberhardt et al., 2005; Eberhardt, 2012). There is substantial prior work on identifiability results and structure learning algorithms that incorporate interventional i.i.d. data for (static) Bayesian networks (Hauser & Bühlmann, 2012; Shanmugam et al., 2015; Yang et al., 2018; Brouillard et al., 2020; Jaber et al., 2020; Ke et al., 2020; Squires et al., 2020). However, we are not aware of prior work in structure learning for dynamic Bayes nets that considers interventional data (potentially along with observational data).

In this paper, we propose a graph structure learning approach for time series data, in the form of dynamic Bayesian networks, while leveraging interventional data in addition to standard observational data. Similar to the case of i.i.d. data, an intervention on time series data requires modifying the process that generates the random variables over time; this is achieved when an experimenter changes conditional distributions of random variables. Note that an intervention can be made for any variable at any time slice in general.

To utilize interventional data, we formulate learning as a continuous optimization problem, extending the recent algebraic characterization of DAGs in time series datasets, known as DYNOTEARS (Pamfil et al., 2020). There are two crucial innovations: 1) While DYNOTEARS applies a new (continuous DAG) constraint to observational linear time series data, we introduce a non-linear objective through neural models, thereby allowing for nonlinear temporal dynamics. 2) We formulate a modified objective and general solution approach that can handle different distributions on intervention targets, thereby vastly expanding the scope of learning to general interventions in time series data.

Our work is closely related to aspects of reinforcement learning (RL) such as factored MDPs (Boutilier et al., 1995), which involve optimizing a target node (reward) in a dynamically evolving process with an underlying graphical model (with partially or fully observable nodes), given control over a subset of nodes (decision/action nodes). In the context of offline RL (Levine et al., 2020), action nodes cannot be actively intervened upon, as only pre-existing data from the

actions (possibly of other agents) are available; however, offline data from multiple policies effectively provides access to different interventions on fixed targets.

Contributions. Our main contributions are as follows:

- We propose a general DBN structure learning algorithm called IDYNO an interventional extension of DYNOTEARS that is capable of utilizing both observational and interventional time series data.
- We extend the baseline IDYNO to nonparametric models for handling potentially complex and nonlinear time series data. The resulting methods can leverage perfect (hard) and imperfect (soft) interventions with known targets.
- We present identifiability results around interventional equivalence classes for our learning approach, under some specified assumptions.
- Through synthetic as well as simulated offline RL datasets, we show that our proposed IDYNO outperforms existing score-based methods by utilizing such interventional data.

2. Background

Consider a set of independent realizations of a stationary time series, with each individual realization of size T in the form of $X_t := [x_{t,i}]_{i=1}^d \in \mathbb{R}^d$. Here $t \in \{0,...,T\}$ represents the time index, X_t represents the observed values of all d number of variables in an observational or interventional time series dataset, and $x_{t,i}$ denotes the i-th component of X_t . We use lower case letters for scalars, upper case letters for vectors, bold letters for matrices. As typically assumed in such models, there may exist instantaneous or contemporaneous influences as well as a time-delayed impact among variables. This is illustrated in the simple DBN in Figure 1.

2.1. Basic Notation

A causal graphical model is defined by a distribution P_X over a set of random variables $X \in \mathbb{R}^d$ and a directed acyclic graph (DAG) $\mathcal{G} = (V, E)$ with nodes V and edges E. Each node $i \in V = \{1, ..., d\}$ is associated with a random variable x_i and each edge $(i, j) \in E$ represents a direct causal relation from variable x_i to x_j . With a slight abuse of notation, we will use X and V interchangeably. We assume the distribution P_X is Markov with respect to graph \mathcal{G} , which enables the factorized joint distribution as $P(X) = \prod_{j=1}^d p_j(x_j|x_{\pi_j^G})$, where π_j^G is the set of parents of node j in the graph \mathcal{G} and x_B denotes the instantiations of a subset of X whose indices are $B \subset V$. We also assume causal sufficiency, i.e., there are no hidden common causes between any pair of variables in X (Peters et al., 2017).

In time series datasets, there are many possible ways to model P_X . We follow the typical setting in recent work (Pamfil et al., 2020), characterizing X through a stan-

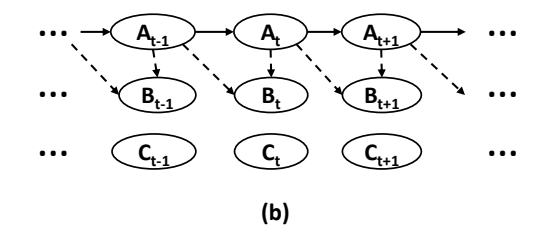


Figure 1. (a) A dynamic Bayesian network (DBN) with 3 nodes: A, B, C. The only intra-slice edges are from A to B and A to C. Note that C has inter-slice edges from the prior two periods whereas A and B have only single period inter-slice edges. (b) DBN from (a) with soft and hard interventions for variables B and C respectively.

dard SVAR model (Demiralp & Hoover, 2003; Swanson & Granger, 1997; Kilian, 2013):

$$X_t = X_t \mathbf{W} + X_{t-1} \mathbf{A_1} + \dots + X_{t-p} \mathbf{A_p} + Z_t,$$
 (1)

where $t \in \{p, ..., T\}$ with horizon T, p is the autoregressive order, and $Z_t \in \mathbb{R}^d$ is a vector of noise variables drawn from any continuous distribution. We assume Z_t is independent of $Z_{t' \neq t}$ and of $X_{t'}$ for all t'. The $d \times d$ matrices \mathbf{W} and \mathbf{A}_i , $i \in \{1, ..., p\}$, represent weighted adjacency matrices for the intra-slice and inter-slice edges in \mathcal{G} , respectively, and model the contemporaneous and time-lagged causal relations. As is typical in dynamic Bayesian networks, \mathbf{W} and \mathbf{A}_i are constrained to ensure that the underlying graph is acyclic; note that inter-slice edges are such that there are only edges from the previous time slice to the current time slice. Eq. 1 can be written in matrix form:

$$\mathbf{X} = \mathbf{X}\mathbf{W} + \mathbf{Y}_1 \mathbf{A}_1 + \dots + \mathbf{Y}_n \mathbf{A}_n + \mathbf{Z}$$
 (2)

where $\mathbf{X} \in \mathbb{R}^{n \times d}$ is a matrix whose rows are $X_t, \mathbf{Z} \in \mathbb{R}^{n \times d}$ is a matrix formed similarly by Z_t , and $\mathbf{Y_j}, j \in \{1,...p\}$, are time lagged versions of \mathbf{X} . The number n is the effective sample size, which is equal to T - p + 1. Let $\mathbf{Y} = [\mathbf{Y_1},...,\mathbf{Y_p}]$ be a matrix with size $n \times pd$ concatenation of time-lagged data, $\mathbf{A} = [\mathbf{A_1}^T,...,\mathbf{A_p}^T]^T$ be a matrix with size $pd \times d$, then the formulation takes the structural equation model (SEM) form:

$$X = XW + YA + Z \tag{3}$$

We refer to such a data transformation as time-lagged, so that it has the same matrix form as i.i.d. data.

2.2. Interventions

An intervention on a variable x_j in a DAG $\mathcal G$ corresponds to replacing its factored conditional distribution $p_j(x_j|x_{\pi_j^G})$ with another distribution $\hat p_j(x_j|x_{\pi_j^G})$. The intervention can be performed on multiple variables simultaneously with a set of interventional targets $I\subseteq V$. Denote the interventional family by $\mathcal I:=(I_1,...,I_K)$, where K is the number

of interventions. The joint likelihood for the kth intervention can be written as:

$$p^{(k)}(X) := \prod_{j \notin I_k} p_j^{(1)}(x_j | x_{\pi_j^G}) \prod_{j \in I_k} p_j^{(k)}(x_j | x_{\pi_j^G})$$
 (4)

The typical intervention on the data from Eq. 4 is referred to as an *imperfect* (or *soft*) intervention. An intervention can also be *perfect* (or *hard*), if it completely removes the dependencies of a node x_j on its parents, 1 for example by setting $p_j^{(k)}(x_j|x_{\pi_j^G})=p_j^{(k)}(x_j), \forall j\in I_k$. Real-world examples of these types of interventions include gene knockouts/knockdowns in biology or performing a fixed action for a decision variable with a deterministic policy in a reinforcement learning environment.

We note that while existing work can handle multiple interventional families, they focus on only one interventional target at a time (Brouillard et al., 2020). Our method in comparison allows for multiple interventions at any time.

2.3. Causal Structure Learning

The goal of typical causal structure learning tasks is to recover the DAG \mathcal{G} using samples from P_X and/or from the interventional distributions. The exact recovery of the graph is typically costly, due to the super-exponential search space in number of nodes, and may not always be identifiable. In Section 1, we mentioned some prior literature on the subject.

The most relevant work here is the following continuous constrained optimization re-formulation for DAG learning that uses a continuous DAG constraint, $h(\mathbf{W}) = 0$ on the weighted adjacency matrix \mathbf{W} to avoid the combinatorial search on the feasible solutions \mathbf{W} (Zhang et al., 2019):

$$\min_{\theta, \mathbf{W}} L_{\theta}(\mathbf{X}; \mathbf{W}) - \lambda \Omega(\theta, \mathbf{W}) \quad s.t. \quad h(\mathbf{W}) = 0, \quad (5)$$

where L_{θ} is the loss function and θ indicates parameters other than \mathbf{W} , $\Omega(\theta, \mathbf{W})$ is a regularization term on model

¹A hard intervention in this sense can be stochastic, and does not necessarily imply deterministically fixing the value of a node.

parameters and/or the edge complexity in \mathbf{W} with a tunable regularization parameter λ . Zhang et al. (2019) propose $h(\mathbf{W}) = \text{Tr}(e^{\mathbf{W}}) - d$, where Tr represents the matrix trace, and shows the graph is acyclic if and only if the constraint $h(\mathbf{W}) = 0$. Typically, the loss f_{θ} can be the least square loss (Zhang et al., 2019) in linear structured equation models (SEM), or evidence lower bound (Yu et al., 2019), among other losses (Kalainathan et al., 2018). The problem is then approximately solved using an augmented Lagrangian procedure. Many extensions to the method have been proposed (Lachapelle et al., 2020; Ng et al., 2019).

For time series datasets, DYNOTEARS (Pamfil et al., 2020) extends the continuous optimization framework to DBNs by explicitly modeling the intra- and inter-slice adjacency matrices separately with a linear SEM model. Namely:

$$\min_{\theta, \mathbf{W}, \mathbf{A}} L_{\theta}(\mathbf{X}; \mathbf{W}, \mathbf{A}) - \lambda \Omega(\theta, \mathbf{W}) \text{ s.t. } h(\mathbf{W}) = 0, (6)$$

where **W** is the matrix for intra-slice edges and **A** is the matrix for inter-slice connections, and $L_{\theta}(\mathbf{X}; \mathbf{W}, \mathbf{A}) = \frac{1}{n}||\mathbf{X} - \mathbf{X}\mathbf{W} - \mathbf{Y}\mathbf{A}||_F^2$. Here n is the total sample size, and $||\cdot||_F$ is the Frobenius norm. To distinguish with the Frobenius norm, we use $||\cdot||_2$ to denote the (vector) l_2 norm.

3. IDYNO: Structure Learning from Interventional Time Series Data

We make two major improvements of the existing graph learning algorithms in the proposed algorithm, IDYNO. First, we propose a new DAG learning method and algorithm that can handle both observational and interventional time series data. Second, we propose to use a more complex nonparametric family of models to capture arbitrary distribution P_X more accurately.

3.1. Time Series Data with Interventions

First, we develop a method that can handle both interventional and observational data together, based on a similar idea from i.i.d. datasets (Brouillard et al., 2020). The main idea is to learn a DAG from interventional data by considering a separate distribution family for the intervened nodes (in the cases of perfect intervention, removing intervened nodes) in the log-likelihood objective. Specifically, in a standard SVAR model, let a binary indicator matrix $\mathbf{R}^{\mathcal{I}} = [r_{kj}^{\mathcal{I}}] \in \{0,1\}^{K \times d}$ encode the interventional family \mathcal{I} , such that $r_{kj}^{\mathcal{I}} = 1$ when x_j is an intervened target in I_k and 0 otherwise. For each interventional family k, we use $\mathbf{W}_{(\mathbf{k})} \in \mathbb{R}^{d \times d}$ and $\mathbf{A}_{(\mathbf{k})} \in \mathbb{R}^{pd \times d}$ to denote the corresponding weighted adjacency matrices, and $\mathbf{W} := \{\mathbf{W}_{(1)}, ..., \mathbf{W}_{(\mathbf{K})}\}$, $\mathbf{A} := \{\mathbf{A}_{(1)}, ..., \mathbf{A}_{(\mathbf{K})}\}$ represent the collection matrices of all interventional families. The loss function $L_{\theta}(\mathbf{X}; \mathbf{W})$ in Eq (6) considers both ob-

servational and interventional data, namely:

$$L_{\theta}(\mathbf{X}; \mathbf{W}, \mathbf{A}) = \sum_{k=1}^{K} \sum_{j=1}^{d} L_{j}(\mathbf{X}; \mathbf{W}_{(1)}, \mathbf{A}_{(1)})^{1 - r_{kj}^{\mathcal{I}}} + L_{j}(\mathbf{X}; \mathbf{W}_{(k)}, \mathbf{A}_{(k)})^{r_{kj}^{\mathcal{I}}}$$
(7)

where L_j denotes the loss associated with the jth component. Then, the optimization becomes:

$$\min_{\mathbf{W}, \mathbf{A}} \frac{1}{n} \sum_{k=1}^{K} \sum_{j=1}^{d} \left(\left| \left(\mathbf{X} - \mathbf{X} \mathbf{W}_{(1)} - \mathbf{Y} \mathbf{A}_{(1)} \right)_{j} \right| \right|_{2}^{2(1 - r_{kj}^{\mathcal{I}})} + \left| \left| \left(\mathbf{X} - \mathbf{X} \mathbf{W}_{(k)} - \mathbf{Y} \mathbf{A}_{(k)} \right)_{j} \right| \right|_{2}^{2r_{kj}^{\mathcal{I}}} \right) + \lambda \Omega(\theta)$$
s.t. $Tr(e^{\mathbf{W}}) - d = 0$ (8

Then the final estimated graph structure would be $\mathbf{W}_{(1)}$ and $\mathbf{A}_{(1)}$, indicating the underlying graph structures under no interventions.

In the case of perfect or hard interventions, intervened nodes no longer depend on W or A, and hence their loss can be removed from the objective without affecting the minimization with respect to W and A.

3.2. Nonlinear Time Series Data

Nonlinear Observational Time Series Data In practice, the relationships among variables can be highly nonlinear, increasing the difficulty in modeling. To alleviate this issue, we first adapt the nonlinear relationships in the continuous constrained optimization DAG learning framework for time series data to the IDYNO framework, with a nonparametric model such as the neural network based NOTEARS method (Zheng et al., 2020). In this class of models, there may not be parameters directly representing the weighted adjacency matrices W and A.

We assume that there exist functions $f_j: \mathbb{R}^d \to \mathbb{R}$ and $g_j: \mathbb{R} \to \mathbb{R}$ such that:

$$\mathbb{E}[x_j|x_{\pi_j^G}] = g_j(f_j(X), f_j^p(Y)), \quad \mathbb{E}[f_j(X)] = 0$$
 (9)

where $f_j(x_1,...,x_d)$ does not depend on x_k if $x_k \notin \pi_j^G$, and f_j^p is the time-lagged function. We assume g_j follows a generalized linear model (GLM) with possible non-additive noise terms. In this work, we study the link function g_j as the sum of two terms. In this setting, we seek to learn $f=(f_1,...,f_d)$ such that the DAG from f, $\mathbf{W}(f)$, represents the same DAG over the data X. The overall objective can be written as:

$$\min_{f} L_{\theta}(f) - \lambda \Omega(\theta) \quad s.t. \quad \mathbf{W}(f) \text{ is a DAG} \qquad (10)$$

where
$$L_{\theta}(f) = \sum_{j=1}^{d} L(X_j, f_j(X), f_j^p(Y)).$$

However, it is not straightforward to directly use a W and A in the parametrization of the neural network, since neural networks do not contain them, and the continuous acyclicity constraint h(W) requires W explicitly. To remedy this problem, we extend the nonparametric acyclicity to time series datasets by using partial derivatives to measure the dependence of each function f_i on the qth variable.

220

221

222

223

224

225

226

227

228

229

230

231

232

233

234

235

236

237

238

239

240

241

242

243

244

245

246

247

248

249

250

251

252

253

254

255

256

257

258

259

261

263

264

265

266

267

269

270

271272

273

274

Let $H^1(\mathbb{R}^d)\subset L_2(\mathbb{R}^d)$ be the Sobolev space of square-integrable functions whose derivatives are also square integrable. Let $f_j\in H^1(\mathbb{R}^d)$ and $\partial_q f_j$ be the partial derivative with respect to x_q . It can be shown that f_j is independent of x_q if and only if $||\partial_q f_j||_{L_2}=0$, where $||\cdot||_{L_2}$ is the usual L_2 -norm. Then each entry of $\mathbf{W}(f)=\mathbf{W}(f_1,...,f_d)\in\mathbb{R}^{d\times d}$ can be defined as:

$$[\mathbf{W}(f)]_{qj} := ||\partial_q f_j||_{L_2}$$

To use a neural network to approximate f_j , we define f_j , for each j, as a multi-layer perceptron (MLP) with h hidden layers and activation $\sigma:\mathbb{R}\to\mathbb{R}$, given by

$$MLP(U;\mathbf{M^{(1)}},...,\mathbf{M^{(h)}}) = \sigma(\mathbf{M^{(h)}}\sigma(...\mathbf{M^{(2)}}\sigma(\mathbf{M^{(1)}}U)))$$

where $\mathbf{M}^{(1)}$ is the (matrix) weight of each layer in MLP. If the qth column of the first layer weight $\mathbf{M}^{(1)}$ consists of all zeros, then $MLP(U; \mathbf{M}^{(1)}, ..., \mathbf{M}^{(h)})$ is independent of u_q , the qth component of U.

The above analysis focuses on one variable x_j at a time. Let $\theta_j = (M_j^{(1)},...,M_j^{(h)})$ denote parameters for the the jth MLP, and $\theta = (\theta_1,...,\theta_d)$. Let $[\mathbf{W}(\theta)]_{qj} = ||q$ th-column $(M_j^{(1)})||_2$ and λ_a,λ_w as the regularization parameters for \mathbf{A} and \mathbf{W} , respectively. Then the overall objective becomes:

$$\min_{\mathbf{W}, \mathbf{A}, \theta} \frac{1}{n} \sum_{j=1}^{d} L_j(\mathbf{X}, \mathbf{MLP}(\mathbf{X}; \theta_j, \mathbf{W}, \mathbf{A}) + \lambda_{\mathbf{a}} ||\mathbf{A}_j^{(1)}||_{1,1}$$

$$+ \lambda_w ||W_i^{(1)}||_{1,1} \quad s.t. \quad \mathbf{W} \text{ is acyclic}$$

where $MLP(X; \theta_j, \mathbf{W}, \mathbf{A})$ produces the estimate \hat{X}_j . Since there are two adjacency matrices \mathbf{W} and \mathbf{A} to be learned, we use separate MLPs for them and concatenate the output from each MLP via a third MLP. In other words, we set $MLP(X; \theta_j, \mathbf{W}, \mathbf{A})$ as the combination of separate MLPs for \mathbf{W} and \mathbf{A} , i.e., $MLP_1(MLP_2(X; \mathbf{A}, \theta_j^A), MLP_3(X; \mathbf{W}, \theta_j^W); \theta_j)$. $\mathbf{A}^{(1)}$ and $\mathbf{W}^{(1)}$ are first layer parameters for \mathbf{W} and \mathbf{A} networks.

Solving the continuous program can be done with any offthe-shelf solver. As typical in the continuous acyclic formulation, the standard augmented Lagrangian transforms the problem into a series of unconstrained objectives;

$$\min_{\theta} L(\theta) + \frac{\rho}{2} |h(\mathbf{W}(\theta))|^2 + \alpha h(\mathbf{W}(\theta))
+ \lambda_a ||A_i^{(1)}||_{1,1} + \lambda_w ||W_i^{(1)}||_{1,1}$$
(11)

To solve the unconstrained l_1 -penalized smooth minimisation problem above, a number of possible optimizers could be used. A natural choice would be the L-BFGS-B algorithm (Byrd et al., 1995). Since Eq (11) is a nonconvex program due to the acyclicity constraint, only a stationary solution can be guaranteed.

Nonlinear Interventional Time Series Data With the above proposal nonparametric model for time series data, we propose a neural network version of IDYNO, denoted as IDYNO-nn, to handle potentially complex nonlinear interventional time series data. The main difference from the observational data is the use of interventional loss functions for each interventional family.

$$\min_{W,A,\theta} \frac{1}{n} \sum_{k=1}^{K} \sum_{j=1}^{d} L_j(\mathbf{X}, MLP(\mathbf{X}; \theta_j, \mathbf{A_{(1)}}, \mathbf{W_{(1)}}))^{1-r_{kj}^{\mathcal{I}}}$$

$$L_j(\mathbf{X}, MLP(\mathbf{X}; \theta_j, \mathbf{A_{(k)}}, \mathbf{W_{(k)}}))^{r_{kj}^{\mathcal{I}}}$$

$$+ \lambda_a ||A_j^{(1)}||_{1,1} + \lambda_w ||W_j^{(1)}||_{1,1}$$
 (12)

$$s.t. \quad Tr(e^{\mathbf{W}}) - d = 0 \tag{13}$$

Eqs (12)-(13) can be solved similarly as (11), to achieve stationary point solutions.

3.3. Identifiability

Identifiability of the DAG structures for observational time series data has been established (Pamfil et al., 2020), where the inter-slice edges represented by A are identified from standard results in vector autoregressive (VAR) models, whereas the intra-slice edges W can be identified under two special cases: 1) the errors Z are non-Gaussian, as a well-known consequence of Marcinkiewicz's theorem and independent component analysis (Pamfil et al., 2020), or 2) all errors Z are standard Gaussian with zero mean and equal variance (Peters & Bühlmann, 2014). For linear time series interventional datasets with known targets, identifiability results have been studied in the i.i.d. case (Chen et al., 2018). Specifically, if each variable is affected by a unique set of intervened variables, the resulting model is identifiable. For time series data, under the (linear) SVAR parametric distribution assumption, one could establish the same identification results, since the reformulation with time-lagged data can be seen as equivalent to an i.i.d. formulation.

With nonlinear interventional data, the identification results above may not apply anymore. However, without further distributional assumptions, Brouillard et al. (2020) establishes identifiability of the \mathcal{I} -Markov equivalent class in i.i.d. data. These results can be extended to IDYNO-nn for time series data in the following fashion.

First, we define a generalized version of \mathcal{I} -Markov equivalence from prior work (Hauser & Bühlmann, 2012; Yang

et al., 2018) for graphs within a (domain or problemdependent) subset of DAGs rather than all DAGs:

Definition 3.1. $((\mathcal{I},\mathcal{D})\text{-Markov}$ **Equivalence Class**). Given a set of interventions \mathcal{I} on a DAG \mathcal{G} in a subset \mathcal{D} of all possible DAGs over a set of variables, we define $(\mathcal{I},\mathcal{D})$ -MEC(\mathcal{G}) as the subset of graphs in \mathcal{D} which are $\mathcal{I}\text{-Markov}$ equivalent to \mathcal{G} .

As such, $(\mathcal{I}, \mathcal{D})$ -MEC (\mathcal{G}) is simply the intersection of \mathcal{D} with the \mathcal{I} -Markov equivalence class of \mathcal{G} , i.e. $\mathcal{D} \cap (\mathcal{I})$ -MEC (\mathcal{G}) . We also define the negative score function $-\mathcal{S}^{\mathcal{I}}(\mathcal{G})$ of a model graph \mathcal{G} as the expectation $\mathbb{E}_{\mathbf{X}|\{p^{(k)}\},\mathcal{G}^{\star}}[L_{\mathrm{reg}}(\mathbf{X})]$ – where L_{reg} is the regularized loss being minimized in Eq. (12) with the losses L_{j} being negative log-likelihoods – over data \mathbf{X} generated from the true graph \mathcal{G}^{\star} with interventional distributions $p^{(k)}$ for each $I_{k} \in \mathcal{I}$.² With these definitions, the following result holds: (Please see the proof and related discussion in Appendix A.)

Theorem 3.2. For a graph $\hat{\mathcal{G}} \in \mathcal{D}$, where $\mathcal{D} \subset DAG$, if $\hat{\mathcal{G}} \in argmax_{\mathcal{G} \in DAG} \mathcal{S}_{\mathcal{I}}(\mathcal{G})$, and furthermore if (i) the density model, i.e. functions $\{g_j, f_j, f_j^p\}$ along with noise terms, has sufficient capacity to exactly represent the ground truth distribution P_X , (ii) a given set of interventions \mathcal{I} satisfies \mathcal{I} -faithfulness for the true graph and distributions $(\mathcal{G}^{\star}, P_X)$, (iii) the density models are strictly positive, and (iv) the ground truth densities $p^{(k)}(\mathbf{X})$ have finite differential entropy, then $\hat{\mathcal{G}}$ is $(\mathcal{I}, \mathcal{D})$ -Markov equivalent to \mathcal{G}^{\star} , for small enough λ_a, λ_w .

Setting \mathcal{D} to be the subset \mathcal{D}_s of DAGs which correspond to stationary dynamics with constant-in-time inter-slice and intra-slice conditional distributions (see Appendix A for details), Theorem 3.2 takes the following form:

Corollary 3.3. For a graph $\hat{\mathcal{G}} \in \mathcal{D}_s$ and given the assumptions mentioned in Theorem 3.2, $\hat{\mathcal{G}}$ is $(\mathcal{I}, \mathcal{D}_s)$ -Markov equivalent to \mathcal{G}^* , for small enough λ_a, λ_w .

Here, restricting to DAGs in \mathcal{D}_s while allowing interventions in \mathcal{I} to change over time reduces the size of the equivalence class $(\mathcal{I}, \mathcal{D}_s)$ -MEC (\mathcal{G}^{\star}) .

4. Empirical Evaluation

We compare the proposed IDYNO methods, including both linear/nonlinear and soft/hard regimes, with baseline methods for time series interventional datasets to show the superior performance of the proposed methods. We first compare different methods on synthetic datasets and then apply them to control tasks to discover the underlying structures. Since there are no known structure learning algorithms for interventional dynamic data, we compare our method to implementations of various state-of-the-art observational baselines, including DYNOTEARS (Pamfil et al., 2020),

standard vector autoregressive models (VAR) (Johansen, 1991), and i.i.d. differential interventional method DCDI (Brouillard et al., 2020). We need to transform time series data for DCDI's usage. We use the following 2-step procedure: 1) fit VAR to compute the residual $\mathbf{e} = \mathbf{Z}(\mathbf{I} - \mathbf{W})^{-1}$ and $\mathbf{B} = \mathbf{A}(\mathbf{I} - \mathbf{W})^{-1}$ and 2) use DCDI to learn \mathbf{W} over the residual data $\mathbf{e} = \mathbf{e}\mathbf{W} + \mathbf{Z}$. This two step approach can learn both the \mathbf{W} and $\mathbf{A} = \mathbf{B}(\mathbf{I} - \mathbf{W})$, although errors can propagate via estimation of earlier steps (Pamfil et al., 2020). All experiments are done in Python on a machine with 3.7GHz CPU and 16GB memory.

4.1. Synthetic Dynamic Datasets

We first evaluate different approaches on synthetic time series data. We simulate the data according to the SEM from Eq (3), mostly following the setup and code from Pamfil et al. (2020) for ease of comparison. The generating process consists of 3 steps:

- 1. Generating weighted graphs in the form W and A.
- Generating data matrices X and corresponding Y per W and A.
- 3. Generating interventional data with random targets and different distributions.

We repeat each experiment 5 times and compare the structural Hamming distance (SHD) between the learned graph and the estimated graph (the lower, the better). We report the mean and the standard error for each case. We generate linear datasets first and then more complex datasets under more difficult settings.

 Table 1. SHD Results for Synthetic Linear Datasets

 Dataset
 DYNOTEARS | IDYNO

 Observational
 2.0 ± 0.0 | 2.0 ± 0.0

 Interventional
 32 ± 0.4 | 19 ± 0.3

Linear Synthetic Interventional Datasets In the linear setting, we use the following steps and hyper-parameters to generate the data.

- For step 1), we use the Erdos-Renyi model to generate intra-slice graph \mathbf{W} with degree of 3 for a total d=10 nodes, with its weights sampled uniformly at random from $\mathcal{U}([-2.0,-0.5]\cup[0.5,2.0])$. We use the same Erdos-Renyi model to generate inter-slice graph \mathbf{A} with degree of 3, with its weights sampled uniformly at random from $\mathcal{U}([-0.5,-0.3]\cup[0.3,0.5])$.
- For step 2), we focus on data with first autoregressive order, i.e., p=1, where data only depends on the previous time slice. We generate 5 sequences with 500 time slices each with standard Gaussian noises. We estimated one graph from each sequence and report the average SHD

²We omit the constraint, Eq. (13), since the theoretical analysis applies to the space of DAGs, and does not consider cyclic graphs.

333 335 337

345

380

381

382

383

384

along with its standard error.

For step 3), to generate interventional data, we flip a fair coin to decide whether to intervene at any time slice, in which case we sample one node uniformly to be the intervened node. Here we deploy a perfect intervention, setting the choosing the values of intervened nodes from $\{0.25, 0.5, 0.75, 1\}$ randomly. The number of intervention families K is therefore 2. We also compare methods for purely observational data (Obs).

As shown in Table 1, the proposed IDYNO method achieves similar accuracy as DYNOTEARS on the observational dataset, validating it can handle observational data. For the interventional dataset, IDYNO significantly outperforms DYNOTEARS, achieving almost half of the SHD.

Nonlinear Interventional Datasets Next we test IDYNO-nn, along with all other baselines, on nonlinear synthetic dynamic datasets. The data generating process is similar to the linear setting, except the underlying function between a node and its parents becomes a two-layer MLP with a sigmoid activation function. In the MLP setting, the weights of the MLPs are sampled uniformly from $\mathcal{U}([-2.0, -0.5] \cup [0.5, 2.0])$, and then weights in the first layer are updated by the parental weights from W and A structures. We also test the effect of varying sizes of node d, from 5 to 20. The interventional data is generated again with the same hard intervention regime as described previously.

As shown in Figure 2, IDYNO and DYNOTEARS suffer due to their linearity assumptions; IDYNO-nn is the most accurate, performing much better than both linear models.

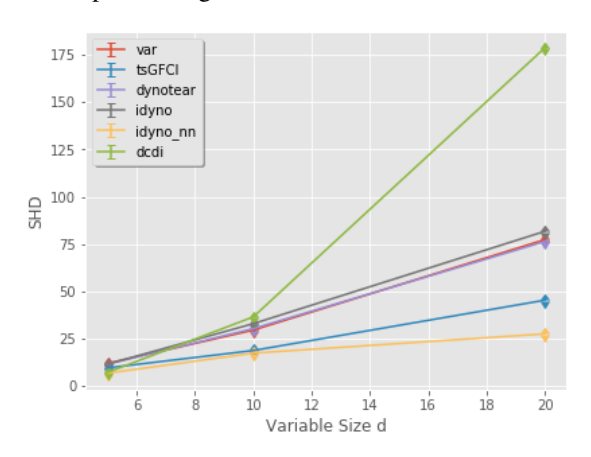


Figure 2. SHD Results for Nonlinear Hard-Intervention Datasets.

Nonlinear Soft-Interventional Datasets Lastly, we also test the methods under soft interventional regimes. We follow the same nonlinear dynamic data generating process as above, with two exceptions: 1) we increase the number of potential interventions at each time slice, and 2) we sample

intervened nodes' values from another distribution. We assume every node has a probability of 0.1 to be intervened upon at each time slice (hence up to d instead of 1), and if a node is chosen, the soft intervention comes from a different 2-layer MLP, depending on the values of its parent nodes per its graph. This soft intervention distribution can be very different from the observation distribution.

As shown by the results in Figure 3, we compare the soft version of the IDYNO-nn, or IDYNO-nn-soft, with all other methods, for $d = \{5, 10, 20\}$. The results confirm that IDYNO-nn is consistently better than DYNOTEARS and IDYNO. IDYNO-nn-soft achieves much better performance than IDYNO-nn, showing that the soft intervention loss function might be necessary in these settings. tsGFCI ranks 2nd, with mean SHD 42.0 against IDYNO-nn-soft 39.0 at d = 20.

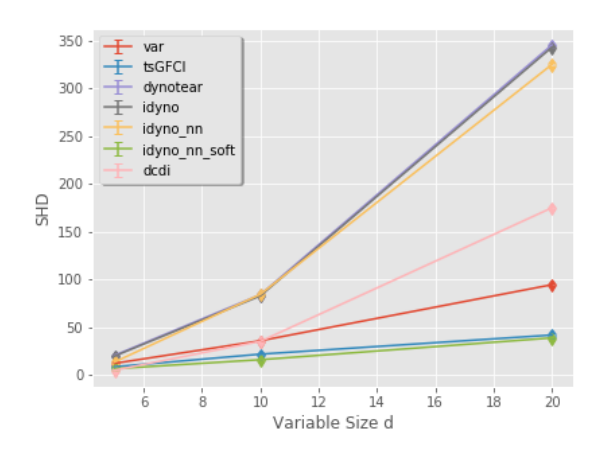


Figure 3. SHD Results for Nonlinear Soft-Intervention Datasets.

4.2. Network Administration Experiments

We consider a network administration example from the factored MDP literature where conditions of computers deteriorate probabilistically based on the underlying network topology (Guestrin et al., 2001). The problem can be modeled as a DBN where the state of each computer depends on its prior state as well as those of its parents in the network and the binary repair action. We consider the continuous state version of the problem where computer conditions are in [0, 1] (Hauskrecht, 2004; Kveton et al., 2006). Details about data generation are in Appendix B. Figure 4 compares results for structure learning of the DBN for a ring network topology with varying number of computers (d). IDYNOnn performs best on this task since it is a hard-intervention dataset; it is better than DYNOTEAR and IDYNO. tsGFCI's performance is closely behind (for example, mean SHD 35.0 against 32.4 at d = 20), possibly due to the limited amount of interventional data.

399

400

401

402

411

412

413

414

415

416

417

418

419

426

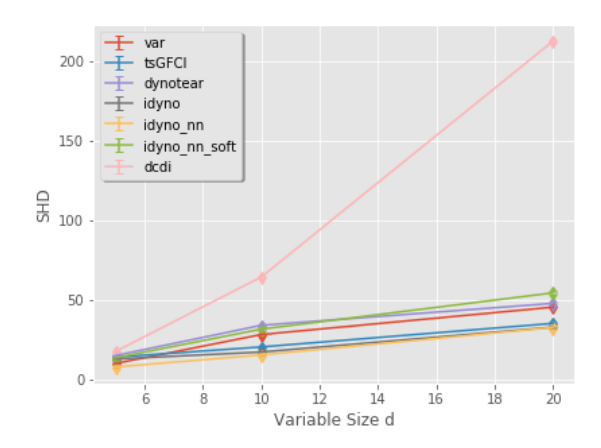


Figure 4. SHD Results for Network Administration Experiments

4.3. Continuous Control Experiments

For these experiments, we apply the proposed methods to a reinforcement learning environment, where data is provided by RL agent actions. We work in the offline RL setting where data trajectories are generated in advance by multiple unknown policies (intervention families k) and are used for structure learning without online acquisition of more data (Sutton & Barto, 2018; Levine et al., 2020).

We use the continuous version of the Lunar Lander environment in OpenAI Gym (Brockman et al., 2016), as DYNOTEARS handles only continuous variables. Lunar Lander is a mini-game where an agent tries to land a lunar lander safely in a desired location without crashing. Let us denote the state and action space dimensionalities as $(d_s, d_a) = (6, 2)$. States η_1 through η_6 are the lander's horizontal position, horizontal velocity, vertical position, vertical velocity, angular orientation, and angular velocity, respectively. Actions β_1 and β_2 are the forces from the main engine and orientation engine. We omit two binary state variables indicating whether the lander legs have landed.

State-action dynamics take the following form:³

$$\Delta \eta_1^{(t)} = \tau \eta_2^{(t)} \quad \Delta \eta_2^{(t)} = \tau \beta_2^{(t)} / M$$
 (14)

$$\Delta \eta_3^{(t)} = \tau \eta_4^{(t)} \quad \Delta \eta_4^{(t)} = \tau (\beta_1^{(t)}/M - g) \eqno(15)$$

$$\Delta \eta_5^{(t)} = \tau \eta_6^{(t)} \quad \Delta \eta_6^{(t)} = \tau \cdot f(\beta_1^{(t)}, \beta_2^{(t)}), \tag{16}$$

where $\Delta \eta_i^{(t)} := \eta_i^{(t+1)} - \eta_i^{(t)}$ and $f(\beta_1, \beta_2)$ is a function which evaluates angular torque on the lander.

Note that the actions' parents (which determine the policy in RL) are missing from the above dynamics, which changes depending on the different learned parents. NNbased agents typically take all states as input in policy networks, hence all states are the parents of each action. In

addition, since the MDP generally contains no intra-slice connection W, we purposely introduce them by removing observed states (keeping only actions) at every other time t-1, t+1, ..., and then treating pairs of adjacent timesteps (t, t+1) as a single timestep. In practice, intra-slice connections could occur if data is missing at some times, such that variables at multiple times must be aggregated to form a complete set of nodes. Hence, there are a total of 4 action variables $\{\beta_1^{(t)}, \beta_2^{(t)}, \beta_1^{(t+1)}, \beta_2^{(t+1)}\}$ at a given time. At a given coarse-grained timestep, all state nodes are still parents of each action node. From the above equation, we can construct the ground truth DBN structure governing the MDP at a fixed policy in this setting.

We use one of the state-of-the-art learners, Deep Deterministic Policy Gradient (DDPG) (Lillicrap et al., 2016), for the policy learning agents. We use two DDPG agents: a randomly initialized DDPG agent (intervention family k = 1), and a fully trained agent with 2e5 total time steps (k=2). We then save 10 different episodes performed by both agents with 1000 time steps as the interventional data. If the lander touched down early, we then remove redundant data with maximal reward values (R = 1). To use the time-lagged transformation, we combine one sequence from each agent to form the data matrix.

Table 2. Continuous Lunar Lander (with Latent States) Results

Alg.	tsGFCI	DYNOTEAR	IDYNO	IDYNO-nn-soft
SHD	27.6 ± 0.1	32.6 ± 0.2	32.2 ± 0.1	$\textbf{27.4} \pm \textbf{0.1}$

We only show selected results in Table 2 due to page restictions. IDYNO-nn-soft performs best here, with tsGFCI slightly behind. For other baselines not shown in the table, IDYNO-nn has SHD of 31.2, DCDI 46.4, and VAR 34.8.

5. Conclusion

In this paper, we have proposed IDYNO – an approach for learning the DAG structure of a dynamic Bayesian network from (dynamic) time series data. IDYNO can handle linear and nonlinear dependencies, observational and interventional data, and perfect and imperfect interventions. To the best of our knowledge, IDYNO is the first such proposed algorithm. We show that under standard assumptions, the underlying graph can be identified at least up to the interventional Markov equivalent class. On various synthetic datasets as well as on a continuous control task, we show that IDYNO consistently outperforms its purely observational counterpart, exhibiting great potential to handle interventional datasets. We have considered passive interventional data in this paper but future work could potentially explore active intervention strategies as well as connections to online RL, based on the proposed approach.

 $^{^3}M$, g, and τ are fixed parameters.

References

440

441

442

443

444

445

446

447

448

449

450

451

452

453

454

455

456

457

458

459

460

461

462

463

464

465

466

467

468

469

470

471

472

473

474

475

476

477

478

479

480

481

482

483

484

485

486

487

488

489

490

491

492

493

494

- Bhattacharjya, D., Subramanian, D., and Gao, T. Proximal graphical event models. In *Advances in Neural Information Processing Systems*, pp. 8136–8145, 2018.
- Boutilier, C., Dearden, R., and Goldszmidt, M. Exploiting structure in policy construction. In *Proceedings of the International Joint Conference on Artificial Intelligence*, pp. 1104–1111, 1995.
- Brockman, G., Cheung, V., Pettersson, L., Schneider, J., Schulman, J., Tang, J., and Zaremba, W. OpenAI Gym. *arXiv preprint arXiv:1606.01540*, 2016.
- Brouillard, P., Lachapelle, S., Lacoste, A., Lacoste-Julien, S., and Drouin, A. Differentiable causal discovery from interventional data. In *Advances in Neural Information Processing Systems*, pp. 21865–21877, 2020.
- Byrd, R. H., Lu, P., Nocedal, J., and Zhu, C. A limited memory algorithm for bound constrained optimization. *SIAM Journal on Scientific Computing*, 16(5):1190–1208, 1995.
- Chen, C., Ren, M., Zhang, M., and Zhang, D. A two-stage penalized least squares method for constructing large systems of structural equations. *Journal of Machine Learning Research*, 19(1):40–73, 2018.
- Chickering, D. M. Optimal structure identification with greedy search. *Journal of Machine Learning Research*, 3: 507–554, 2002.
- Colombo, D., Maathuis, M. H., Kalisch, M., and Richardson, T. Learning high-dimensional directed acyclic graphs with latent and selection variables. *The Annals of Statistics*, 40(1):294–321, 2012.
- Dahlhaus, R. Graphical interaction models for multivariate time series. *Metrika*, 51:157–172, 2000.
- Dean, T. and Kanazawa, K. A model for reasoning about persistence and causation. *Computational Intelligence*, 5: 142–150, 1989.
- Demiralp, S. and Hoover, K. D. Searching for the causal structure of a vector autoregression. *Oxford Bulletin of Economics and Statistics*, 65:745–767, 2003.
- Didelez, V. Graphical models for marked point processes based on local independence. *Journal of the Royal Statistical Society, Ser. B*, 70(1):245–264, 2008.
- Eberhardt, F. Almost optimal intervention sets for causal discovery. In *Conference on Uncertainty in Artificial Intelligence*, pp. 161–168, 2012.

- Eberhardt, F., Glymour, C., and Scheines, R. On the number of experiments sufficient and in the worst case necessary to identify all causal relations among N variables. In *Conference on Uncertainty in Artificial Intelligence*, pp. 178–184, 2005.
- Eichler, M. *Graphical Models in Time Series Analysis*. PhD thesis, University of Heidelberg, Germany, 1999.
- Guestrin, C., Koller, D., and Parr, R. Max-norm projections for factored MDPs. In *Conference on Uncertainty in Artificial Intelligence*, pp. 673–682, 2001.
- Gunawardana, A., Meek, C., and Xu, P. A model for temporal dependencies in event streams. In *Advances in Neural Information Processing Systems*, pp. 1962–1970, 2011.
- Hauser, A. and Bühlmann, P. Characterization and greedy learning of interventional Markov equivalence classes of directed acyclic graphs. *Journal of Machine Learning Research*, 13(1):2409–2464, 2012.
- Hauskrecht, Milos, . K. B. Linear program approximations for factored continuous-state markov decision processes. In *Advances in Neural Information Processing Systems*, pp. 895–902, 2004.
- Heckerman, D., Geiger, D., and Chickering, D. M. Learning Bayesian networks: The combination of knowledge and statistical data. *Machine Learning*, 20:197–243, 1995.
- Jaber, A., Kocaoglu, M., Shanmugam, K., and Bareinboim, E. Causal discovery from soft interventions with unknown targets: Characterization and learning. In Advances in Neural Information Processing Systems, pp. 9551–9561, 2020.
- Johansen, S. Estimation and hypothesis testing of cointegration vectors in gaussian vector autoregressive models. *Econometrica: journal of the Econometric Society*, pp. 1551–1580, 1991.
- Kalainathan, D., Goudet, O., Guyon, I., Lopez-Paz, D., and Sebag, M. SAM: Structural agnostic model, causal discovery and penalized adversarial learning. arXiv preprint arXiv:1803.04929, 2018.
- Ke, N. R., Bilaniuk, O., Goyal, A., Bauer, S., Larochelle, H., Schölkopf, B., Mozer, M. C., Pal, C., and Bengio, Y. Learning neural causal models from unknown interventions, 2020.
- Kilian, L. Structural vector autoregressions. In *Handbook of Research Methods and Applications in Empirical Macroe-conomics*. Edward Elgar Publishing, 2013.
- Koller, D. and Friedman, N. *Probabilistic Graphical Models: Principles and Techniques*. MIT Press, 2009.

Kveton, B., Hauskrecht, M., and Guestrin, C. Solving
 factored MDPs with hybrid state and action variables.
 Journal of Artificial Intelligence Research, pp. 153–201,
 2006.

- Lachapelle, S., Brouillard, P., Deleu, T., and Lacoste-Julien, S. Gradient-based neural DAG learning. In *International Conference on Learning Representations*, 2020.
 - Lanne, M., Meitz, M., and Saikkonen, P. Identification and estimation of non-Gaussian structural vector autoregressions. *Journal of Econometrics*, 196(2):288–304, 2017.
 - Levine, S., Kumar, A., Tucker, G., and Fu, J. Offline reinforcement learning: Tutorial, review, and perspectives on open problems. *arXiv preprint arXiv: arXiv:2005.01643*, 2020.
 - Lillicrap, T. P., Hunt, J. J., Pritzel, A., Heess, N., Erez, T., Tassa, Y., Silver, D., and Wierstra, D. Continuous control with deep reinforcement learning. In *International Conference on Learning Representations*, 2016.
 - Linzner, D., Schmidt, M., and Koeppl, H. Scalable structure learning of continuous-time Bayesian networks from incomplete data. *Advances in Neural Information Processing Systems*, 32:3746–3756, 2019.
 - Malinsky, D. and Spirtes, P. Learning the structure of a nonstationary vector autoregression. In *International Conference on Artificial Intelligence and Statistics*, pp. 2986–2994, 2019.
 - Meek, C. Toward learning graphical and causal process models. In *Proceedings of Uncertainty in Artificial Intelligence Workshop Causal Inference: Learning and Prediction*, pp. 43–48, 2014.
 - Meng, Z., Han, S., Liu, P., and Tong, Y. Improving speech related facial action unit recognition by audiovisual information fusion. *IEEE Transactions on Cybernetics*, 49(9): 3293–3306, 2018.
 - Murphy, K. *Dynamic Bayesian Networks: Representation, Inference and Learning*. PhD thesis, University of California Berkeley, USA, 2002.
 - Ng, I., Fang, Z., Zhu, S., Chen, Z., and Wang, J. Masked gradient-based causal structure learning. *arXiv* preprint *arXiv*:1910.08527, 2019.
 - Nodelman, U., Shelton, C. R., and Koller, D. Continuous time Bayesian networks. In *Proceedings of Conference on Uncertainty in Artificial Intelligence*, pp. 378–378, 2002.
 - Oates, C. J., Smith, J. Q., and Mukherjee, S. Estimating causal structure using conditional dag models. *Journal of Machine Learning Research*, 17(1):1880–1903, 2016.

- Pamfil, R., Sriwattanaworachai, N., Desai, S., Pilgerstorfer, P., Georgatzis, K., Beaumont, P., and Aragam, B. DYNOTEARS: Structure learning from time-series data. In *International Conference on Artificial Intelligence and Statistics*, pp. 1595–1605, 2020.
- Pearl, J. *Probabilistic Reasoning in Intelligent Systems*. Morgan Kaufmann, 1988.
- Pearl, J. Causality: Models, Reasoning and Inference. Cambridge University Press, New York, NY, USA, 2nd edition, 2009.
- Peters, J. and Bühlmann, P. Identifiability of Gaussian structural equation models with equal error variances. *Biometrika*, 101(1):219–228, 2014.
- Peters, J., Janzing, D., and Schölkopf, B. *Elements of Causal Inference: Foundations and Learning Algorithms*. The MIT Press, 2017.
- Rajapakse, J. C. and Zhou, J. Learning effective brain connectivity with dynamic Bayesian networks. *Neuroimage*, 37(3):749–760, 2007.
- Reale, M. and Wilson, G. T. Identification of vector ar models with recursive structural errors using conditional independence graphs. *Statistical Methods and Applications*, 10(1-3):49–65, 2001.
- Reale, M. and Wilson, G. T. The sampling properties of conditional independence graphs for structural vector autoregressions. *Biometrika*, 89(2):457–461, 2002.
- Shanmugam, K., Kocaoglu, M., Dimakis, A. G., and Vishwanath, S. Learning causal graphs with small interventions. In *Advances in Neural Information Processing Systems*, pp. 3195–3203, 2015.
- Spirtes, P., Glymour, C., and Scheines, R. *Causality, Prediction, and Search*. MIT Press, Cambridge, MA, USA, 2nd edition, 2001.
- Squires, C., Wang, Y., and Uhler, C. Permutation-based causal structure learning with unknown intervention targets. In *Uncertainty in Artificial Intelligence*, pp. 1039–1048, 2020.
- Sutton, R. S. and Barto, A. G. *Reinforcement Learning: An Introduction*. The MIT Press, second edition, 2018.
- Swanson, N. R. and Granger, C. W. Impulse response functions based on a causal approach to residual orthogonalization in vector autoregressions. *Journal of the American Statistical Association*, 92(437):357–367, 1997.
- Tank, A., Fox, E. B., and Shojaie, A. Identifiability and estimation of structural vector autoregressive models for subsampled and mixed-frequency time series. *Biometrika*, 106(2):433–452, 2019.

Tsamardinos, I., Brown, L. E., and Aliferis, C. F. The maxmin hill-climbing Bayesian network structure learning algorithm. *Machine Learning*, 65(1):31–78, 2006.

- Yang, K., Katcoff, A., and Uhler, C. Characterizing and learning equivalence classes of causal DAGs under interventions. In *International Conference on Machine Learning*, pp. 5541–5550, 2018.
- Yu, Y., Chen, J., Gao, T., and Yu, M. DAG-GNN: DAG structure learning with graph neural networks. In *International Conference on Machine Learning*, pp. 7154–7163, 2019.
- Zhang, A., Lipton, Z. C., Pineda, L., Azizzadenesheli, K., Anandkumar, A., Itti, L., Pineau, J., and Furlanello, T. Learning causal state representations of partially observable environments. *arXiv preprint arXiv:1906.10437*, 2019.
- Zheng, X., Aragam, B., Ravikumar, P. K., and Xing, E. P. DAGs with NO TEARS: Continuous optimization for structure learning. In *Advances in Neural Information Processing Systems*, pp. 9472–9483, 2018.
- Zheng, X., Dan, C., Aragam, B., Ravikumar, P. K., and Xing, E. P. Learning sparse nonparametric DAGs. In *International Conference on Artificial Intelligence and Statistics*, pp. 3414–3425, 2020.

A. Identifiability

In this section we clarify the quantities and notation used in Section 3.3 to establish conditions for identifiability of the "unrolled," temporally extended DAG which includes all variables at all timesteps. We define $\mathbf{X} \in \mathbb{R}^{n \times d}$ (where n = T - p + 1) – as in the main text – as the matrix whose elements form the set of random variables in a DAG $\mathcal{G}^{\star} = (V, E)$, where $V = \{x_{t,i}\}$ for $i \in \{1,...,d\}$ and $t \in \{1,...,n\}$ is the set of indices for d variables across n timesteps, and $(x_{t,i},x_{t',j}) \in E$ if $x_{t,i}$ is an element of the parent nodes $\pi^{\mathcal{G}^{\star}}_{x_{t',j}}$ of $x_{t',j}$. Due to the acyclicity of intra-slice connections and the forward-in-time direction of inter-slice connections, \mathcal{G}^{\star} is directed and acyclic.

We assume that the inter-slice and intra-slice edges in \mathcal{G}^{\star} are constant in time, in the sense that (i) inter-slice edges connecting a given pair of variables $(x_{t,i},x_{t',j})$ with a given time lag p=t'-t are either elements of E for all $p\leq t_2\leq n$ or for no t_2 , and (ii) intra-slice edges $(x_{t,i},x_{t',j})$ connecting a pair of variables at time t are either elements of E for all t or for no t. Furthermore, we assume that the distribution P_X over variables in this graph is invariant across time. That is, we restrict the conditional distribution $p_j(x_{t,j}|\pi_{x_{t,j}}^G)$ for any x_j to be independent of the time index t. We will denote the subset of all DAGs that can be partitioned in this way into a directed sequence of a repeated subgraph as \mathcal{D}_s , in reference to the fact that repetition of the same conditional distributions and edges over time corresponds to stationary or fixed dynamics.

We consider a family of interventions \mathcal{I} on the temporally extended graph \mathcal{G}^{\star} . An intervention $I_k \in \mathcal{I}$ need not modify conditional distributions in the same way at all times, but may modify conditional distributions for any subset of edges $(x_{t,i}, x_{t',j}) \in E$. (Our algorithm IDYNO assumes a smaller subset of interventions which are constant in time, and can thus be viewed as a special choice of \mathcal{I} .)

With these definitions, along with those given in Section 3.3, our dynamical graphical setting reduces to the non-dynamical graphical setting of Brouillard et al. (2020) and we can apply their Theorem 1 to the DAG \mathcal{G}^* as follows.

Proof of Theorem 1. We refer the reader to Brouillard et al. (2020) for precise statements of assumptions (i)-(iv) as stated in Theorem 3.2. When these assumptions ho9ld, Theorem 1 of Brouillard et al. (2020) applies. Thus, as long as λ_a, λ_w are sufficiently close to zero (such that the score $\mathcal{S}_{\mathcal{I}}(\mathcal{G})$ is equivalent to the log-likelihood score in Eq. (8) of Brouillard et al. (2020) in the $\lambda \to 0$ limit), $\hat{\mathcal{G}}$ is \mathcal{I} -Markov equivalent to \mathcal{G}^* . Since furthermore $\hat{\mathcal{G}} \in \mathcal{D}$, then by Definition 3.1, $\hat{\mathcal{G}}$ is $(\mathcal{I}, \mathcal{D})$ -Markov equivalent to \mathcal{G}^* .

B. Network Administration Example

In the network administration example from the factored MDP literature (Guestrin et al., 2001), a cluster of computers are connected together in some underlying network topology such that failures of these computers propagate probabilistically through network connections. The administrator can prevent failure propagation by fixing computers that have failed. The problem can be modeled as a DBN where there is a variable X_i for every computer i in the network. X_i at any epoch depends on its state at the previous period, its parent computer states in the underlying topology (representing the physical dependencies in the network) as well as the binary action performed for the computer, i.e. whether it is repaired or not. At most one computer can be repaired at any epoch due to resource constraints.

In the original version of the problem, variables X_i are binary such that 0 and 1 represent failure and operational states respectively. We consider the continuous state version of the problem where the states of each computer are values between 0 and 1; a lower value indicates a poorer condition (Hauskrecht, 2004; Kveton et al., 2006).

We consider the ring network topology involving d computers, similar to prior work, where there are only edges from computer i to computer i + 1, $i = 1, \dots, d - 1$ as well as an edge from computer d to computer 1. We note that our data generation applies to any network topology in general. Our approach for the DBN sampling follows prior work (Hauskrecht, 2004; Kveton et al., 2006), described as follows.

Action A_i is 1 if the computer indexed i is fixed at any epoch; otherwise it is 0. For the experiments, we consider the realistic policy where only the worst state computer from the previous epoch is fixed. The transition model captures the propagation of failures in the network and is encoded locally by beta distributions with parameters a and b. Specifically, when $A_i = 1$, the state X_i is generated from a beta distribution with the parameters a = 20 and b = 2. In contrast, when

 $A_i = 0$, X_i depends on variables from the previous epoch with the following beta distribution parameters:

$$a = 2 + 13x'_i - \left(2x'_i \sum_{j \in Pa(X_i)} x'_j\right); \quad b = 10 - 2x'_i - \left(2x'_i \sum_{j \in Pa(X_i)} x'_j\right),$$

where x_i' is the state of computer i from the previous epoch, x_j' is the state of computer j from the previous epoch, and $Pa(X_i)$ are the parents of X_i in the network topology. We also enforce non-negativity constraints on the beta parameters above. In this fashion, failures are propagated when a computer is not fixed.